

# Effect of multivalent cations on agglomeration of Ru clusters supported on Y zeolite

Sung June Cho <sup>a,\*</sup>, Jae Eui Yie <sup>b</sup> and Ryong Ryoo <sup>a</sup>

<sup>a</sup> Materials Chemistry Laboratory (School of Molecular Science, BK-21), Korea Advanced Institute of Science and Technology, Taeduk Science Town, Taejeon 305-701, Korea

E-mail: sjcho@kier.re.kr

<sup>b</sup> Division of Chemical Engineering and Biotechnology, Ajou University, Suwon 441-749, Korea

Received 9 June 2000; accepted 14 November 2000

The effect of multivalent cations, Ca<sup>2+</sup>, Ba<sup>2+</sup>, Y<sup>3+</sup>, Ce<sup>3+</sup> and La<sup>3+</sup> on the agglomeration of Ru clusters on NaY zeolite under oxygen and at high temperature has been investigated with <sup>129</sup>Xe NMR spectroscopy and X-ray absorption fine structure. Multivalent metal cations exchanged into the zeolite suppress neither the migration nor agglomeration of small Ru clusters inside the supercage of NaY zeolite into large metal particles onto the external surface of NaY zeolite under 1 atm oxygen above 520 K. However, the resultant Ru particle size depends on the type of metal cations exchanged into NaY zeolite.

**KEY WORDS:** Ru catalyst; <sup>129</sup>Xe NMR; EXAFS; XANES; NaY zeolite; metal cluster; sintering

## 1. Introduction

The effect of multivalent cations on metal catalysts can be found in the growth of the metal particles, their catalysis, etc. Multivalent cations, Ca<sup>2+</sup>, Y<sup>3+</sup>, etc., exchanged into NaY or NaX zeolites have been reported to anchor mobile Pd metal atoms to form 1 nm Pd clusters in the zeolite supercages; otherwise 2 nm Pd clusters are obtained, which occupy a few adjacent supercages [1]. They can also alter the performance of the catalyst as Lewis acid sites. Special attention has been paid to improve the stability and the activity of Ru and Rh catalysts supported on a non-reducible metal oxide. BaO was added to Ru catalysts in order to inhibit the loss of volatile Ru metal oxide under ambient conditions [2].

Cho et al. investigated the reduction–oxidation behavior of Ru metal clusters supported on NaY zeolite [3]. Small Ru clusters of 1 nm inside the supercages of NaY zeolite agglomerate into large bulk Ru metal crystallites (100 nm × 20 nm) on the exterior surface of NaY zeolite crystal when it is heated above 520 K under oxygen atmosphere. Such an oxidation behavior was also reported by Verdonck et al. [4]. Agglomeration of small Ru clusters into large metal crystallites causes the loss of catalytically active sites, resulting in lower catalytic performance.

Thus, it is worthwhile to investigate the effect of multivalent cations on the agglomeration of small Ru clusters under oxygen. In the present work, we probe the effect of multivalent metal cations on the agglomeration of small Ru clusters after heating in 1 atm O<sub>2</sub> atmosphere with <sup>129</sup>Xe NMR spectrum and extended X-ray absorption fine structure (EXAFS).

\* To whom correspondence should be addressed. Present address: Catalytic Combustion Research Team, Korea Institute of Energy Research, 71-2, Jang-dong, Yusung-gu, Taejeon 305-343, Korea.

## 2. Experimental

The experimental procedures used here for sample preparation are the same as those in our previous work on Ru/NaY [3,5]. NaY zeolite was synthesized according to a hydrothermal procedure using Ludox (HS40, Du Pont) as a silica source. Multivalent cations are exchanged into the synthesized NaY zeolite according to the following procedure with Ca(NO<sub>3</sub>)<sub>2</sub>·4H<sub>2</sub>O (Aldrich, 99%), Ba(NO<sub>3</sub>)<sub>2</sub> (Aldrich, 99+%), Y(NO<sub>3</sub>)<sub>3</sub>·4H<sub>2</sub>O (Aldrich, 99.99%), La(NO<sub>3</sub>)<sub>3</sub>·6H<sub>2</sub>O (Aldrich, 99.99%) and Ce(NO<sub>3</sub>)<sub>3</sub>·6H<sub>2</sub>O (Aldrich, 99.999%). NaY zeolite was slurred in the aqueous solution containing a 2.5 times excess amount of multivalent cations for the maximum ion-exchange level of NaY zeolite overnight at room temperature. The solid was collected by filtration. To obtain the maximum ion-exchange level in NaY zeolite the above procedure was repeated twice.

The obtained zeolite powder was slurred in aqueous ammonia solution (100 ml g<sup>-1</sup> zeolite) of RuCl<sub>3</sub> (Johnson Matthey, 48.73%) for 72 h at 330 K. Ultraviolet absorption spectra of the supernatant solution indicated that practically all Ru red complex was ion exchanged from solution to zeolite during this period. The zeolite was filtered, washed with doubly distilled water, and dried in a vacuum oven at RT. This sample was activated inside a Pyrex, U-tube, flow reactor by heating linearly to 673 K over 4 h and maintaining at this temperature for 2 h under vacuum. The sample was then reduced in flowing H<sub>2</sub> (99.999%, passed through a MnO/SiO<sub>2</sub> trap, >200 ml min<sup>-1</sup> g<sup>-1</sup>) with linear heating to 623 K over 4 h and maintaining at this temperature for 2 h. Desorption of chemisorbed hydrogen from the surface of the Ru cluster was performed by increasing the temperature to 673 K over 2 h under 1 × 10<sup>-3</sup> kPa and maintaining under

this condition for 1 h. These samples were used *in situ*, or exposed to air at room temperature. The heat treatment of the Ru catalyst was performed under static 1 atm O<sub>2</sub> for 1 h. The oxidized catalyst sample was reduced again with hydrogen flow at 623 K, for further experiments. The samples are designated as Ru/MY where the number of Ru atoms per unit cell was 6.2 from the chemical analysis and M for the exchanged multivalent cations.

Natural xenon gas (Matheson, 99.995%) was used for the <sup>129</sup>Xe NMR experiment. For the <sup>129</sup>Xe NMR experiment, the sample powder was transferred from the U-tube reactor to a joined NMR tube and sealed off with a flame. The NMR tube was equipped with high-vacuum stopcocks, through which xenon gas was equilibrated with the sample at 296 K under given pressures. <sup>129</sup>Xe NMR spectra were obtained at 296 K with a Bruker AM 300 instrument operating at 83.0 MHz for <sup>129</sup>Xe with a 0.5 s relaxation delay. The chemical shift is referenced to xenon gas extrapolated to zero pressure.

For EXAFS, sample powder weighing 0.20 g was pressed into a self-supporting wafer of 10 mm in diameter for Ru/MY. The sample wafer was treated by the same method as used above for the preparation of Ru cluster in Y zeolite supercage, using a Pyrex reactor. The sample wafer was transferred *in situ* into a joined EXAFS cell. Kapton (Du Pont, 125 μm) windows were glued to the EXAFS cell using Torr Seal (Varian) for the X-ray absorption measurement. The EXAFS cell under H<sub>2</sub> atmosphere was sealed off with a flame. The EXAFS spectra were measured above the Ru K edge by using beamline 10B at the Photon Factory in Tsukuba. A Si(311) channel cut was used to monochromatize the X-ray beam. The beam injection energy was 2.5 GeV, and the ring current was maintained as 300–350 mA. Incident and transmitted X-ray intensities were measured using ionization chambers filled with 100% Ar and 100% Kr, respectively. The X-ray energy ( $\Delta E/E = 1.0 \times 10^{-4}$ ) around the Ru K edge region increased in steps of 0.5 eV and for the EXAFS region in steps of 2.5 eV.

### 3. Results and discussion

The formation and growth of Ru clusters supported on NaY zeolite has been studied using the Xe adsorption method [3]. The heat of Xe adsorption on the Ru cluster in the supercage of NaY zeolite is so large,  $\sim 10$  kcal mol<sup>-1</sup> that the interaction between Xe and Ru cluster caused a large chemical shift change in the <sup>129</sup>Xe NMR spectrum. <sup>129</sup>Xe NMR spectroscopy can probe the physicochemical environment in the supercage since Xe atom, 0.43 nm, can enter only the supercage, 1.3 nm, through the pore aperture, 0.74 nm. The sodalite cage is inaccessible for Xe atom due to the smaller pore aperture size, 0.22 nm. Also, the interaction between <sup>129</sup>Xe atom and the external surface of the NaY zeolite crystal is found to be negligible [6]. Thus, the <sup>129</sup>Xe NMR chemical shift shows mainly the change in the environment of the supercage where the metal cluster forms and grows with various heat treatments [7].

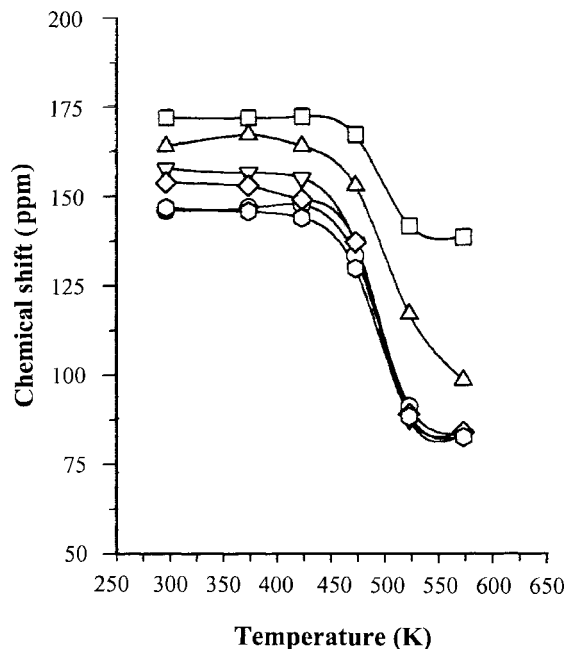


Figure 1. <sup>129</sup>Xe NMR chemical shift of Xe adsorbed on the Ru catalyst at 296 K and 40 kPa. (○) Ru/NaY, (□) Ru/BaY, (△) Ru/CaY, (▽) Ru/LaY, (◇) Ru/CeY and (○) Ru/Y.

The cation-exchanged NaY zeolite has been studied extensively using <sup>129</sup>Xe NMR spectroscopy. It was reported that all the La<sup>3+</sup> and Ce<sup>3+</sup> cations exchanged in NaY zeolites migrate to the hexagonal prism and the sodalite cages when the zeolite was completely dehydrated [8]. While, Pak and Ryoo reported the strong adsorption of Xe atom on Ca<sup>2+</sup> and Ba<sup>2+</sup> cations exchanged into NaY zeolite [9]. This significant interaction between Xe atom and the cations present in the supercage caused a large chemical shift compared to that of the pure NaY. Further, it was suggested that the strong interaction between Xe atom and cation can be used to count the number of the cations present in the supercage.

Figure 1 shows the change of the <sup>129</sup>Xe NMR chemical shift as a function of heating temperature in O<sub>2</sub>. In the previous report, the strong Xe adsorption decreased drastically with the increase of the oxidation temperature [3]. Further, the transmission electron micrograph shows the formation of worm-like bulk Ru metal at the outer surface of zeolite crystallites. The change of the <sup>129</sup>Xe NMR chemical shift for Ru/NaY was consistent with the migration of the Ru cluster as reported earlier. As the Ru cluster in the supercage sintered to form bulk Ru metal particles at the external surface of NaY zeolite, the chemical shift dropped suddenly at around 500 K. The <sup>129</sup>Xe NMR chemical shift for the Ru/NaY sintered at 573 K was the same as that of pure NaY.

After the oxidation at 573 K, the <sup>129</sup>Xe NMR chemical shift in La<sup>3+</sup>, Ce<sup>3+</sup> and Y<sup>3+</sup> cations exchanged NaY zeolites falls to that of the pure NaY zeolite because all cations existed in either the hexagonal prism or sodalite cage. The <sup>129</sup>Xe NMR chemical shift in Ca<sup>2+</sup> and Ba<sup>2+</sup> cations exchanged NaY zeolites was the same as that of the pure

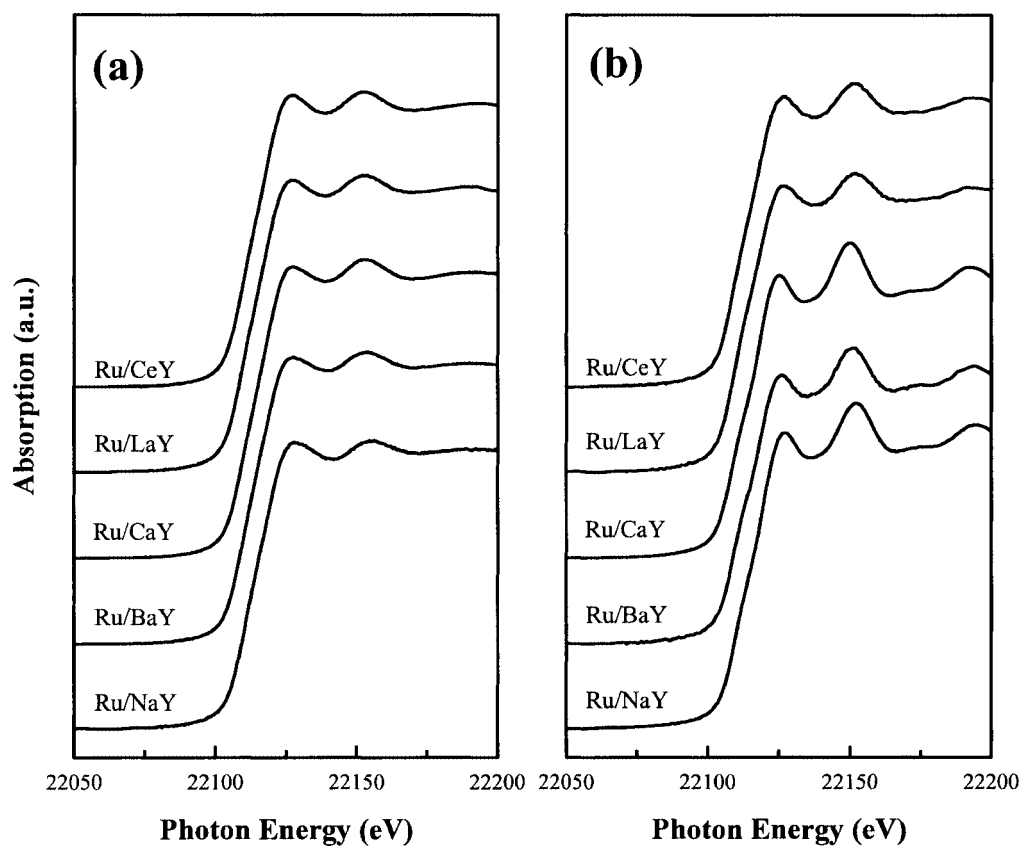


Figure 2. X-ray absorption near-edge spectra of the Ru catalysts (a) before and (b) after the oxidation in 1 atm O<sub>2</sub> at 573 K. For XANES/EXAFS measurement, the oxidized catalyst sample was reduced with hydrogen flow at 623 K.

BaY and CaY, respectively, due to the significant interaction between Xe atom and the cations present in the supercage, which was consistent with the previous report by Pak and Ryoo [9]. Thus, the results suggested that the Ru metal cluster independent of the exchanged cation type migrate out of the supercage of NaY zeolite at the same oxidation temperature leaving the empty supercage.

The results of the Xe adsorption measurement, hydrogen chemisorption indicated that the Ru cluster size was less than 1 nm consisting of 30–40 atoms per cluster independent of the multivalent cations. The La<sup>3+</sup>- and Ce<sup>3+</sup>-exchanged Ru catalysts show a small increase of the <sup>129</sup>Xe NMR chemical shift compared to that in Ru/NaY. It was believed that the surface electronic structure of the Ru cluster was modified a little by the multivalent cation, affecting the interaction between Xe and the surface of the cluster. However, the X-ray absorption near-edge spectra (XANES) of the fresh Ru catalysts in figure 2(a) show no significant change depending on the multivalent cations, which can be attributed to the suppressed absorption transition by the dipole-forbidden transition, 1s → 4d at the Ru K edge.

After the oxidation at 573 K, there is a little difference in the XANESs, as shown in figure 2(b), for the La<sup>3+</sup>- and Ce<sup>3+</sup>-exchanged NaY zeolites compared to those of the Ba<sup>2+</sup>- and Ca<sup>2+</sup>-exchanged NaY zeolites. The structure at the X-ray absorption edge was indicative of the change of coordination geometry, oxidation state, etc. The normalized

Table 1  
Structural parameters obtained from the curve fitting of the EXAFS spectrum above the Ru K edge.

	Before oxidation <sup>a</sup>			After oxidation at 573 K <sup>b</sup>		
	<i>N</i>	<i>R</i> (nm)	$\sigma^2$ (pm <sup>2</sup> ) <sup>c</sup>	<i>N</i>	<i>R</i> (nm)	$\sigma^2$ (pm <sup>2</sup> ) <sup>c</sup>
Ru/NaY	6.1	0.257	81	12.0	0.267	50
Ru/CaY	6.0	0.254	82	12.0	0.267	46
Ru/BaY	5.4	0.255	80	11.4	0.267	44
Ru/LaY	5.3	0.255	66	7.1	0.266	70
Ru/CeY	5.6	0.256	73	6.8	0.266	66

<sup>a</sup> In hydrogen atmosphere.

<sup>b</sup> For EXAFS measurement, all the catalyst sample was reduced with hydrogen flow at 623 K.

<sup>c</sup> The Debye–Waller factor.

maximum peak intensity can be affected with the change of electronic structure like the extent of the d–sp hybridization or the increase of the cluster size. The smaller transition intensity for the La<sup>3+</sup>- and Ce<sup>3+</sup>-exchanged Ru catalysts compared to those of the Ba<sup>2+</sup>- and Ca<sup>2+</sup>-exchanged Ru catalysts may come from the smaller Ru cluster size [5].

Table 1 shows the structural parameters of the Ru catalyst obtained from the curve fitting of EXAFS spectrum using XFIT [10] and FEFF6.01 [11]. In the curve fit, the model EXAFS spectrum was fitted to the experimental EXAFS spectrum in the range of 30–130 nm<sup>-1</sup> in *k*-space and 0.15–0.30 nm in *r*-space. The best model fit was determined

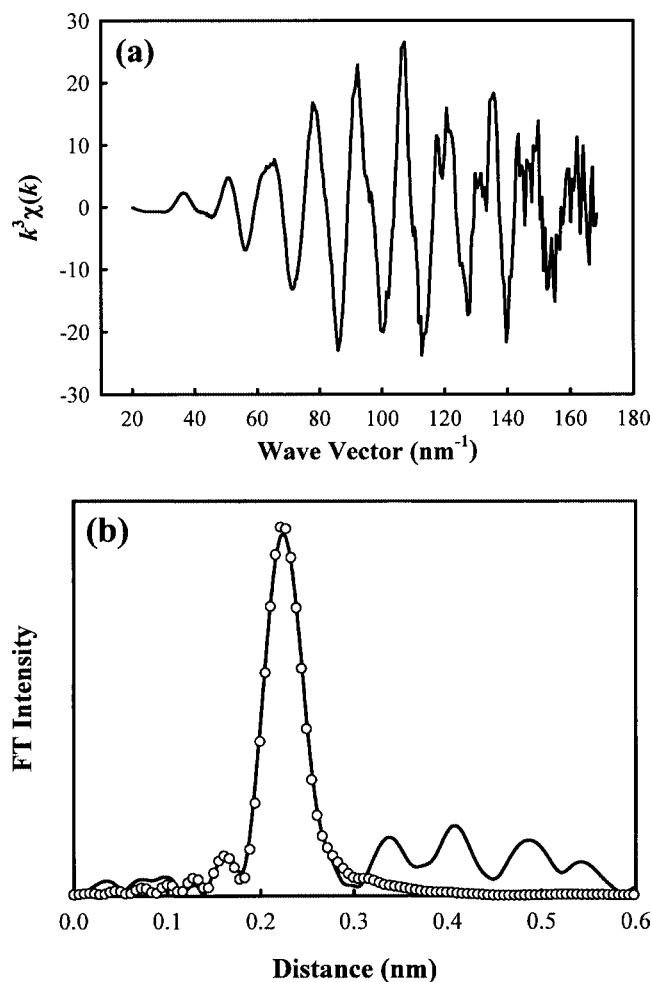


Figure 3. Typical  $k^3$ -weighted EXAFS spectrum and its corresponding Fourier transform of the Ru catalyst. The circles indicate the best fit of the EXAFS function generated from FEFF6.01.

by minimizing the  $R$  factor. The typical EXAFS spectrum and the Fourier transform are shown in figure 3.

All the fresh Ru catalysts have a Ru–Ru coordination number of  $5.7 \pm 0.5$  at  $0.255 \pm 0.001$  nm. Assuming the maximum space filling cluster structure, the obtained coordination number corresponded to 15–20 atoms per cluster. The estimation of the coordination number can be biased due to the presence of the anharmonic thermal vibration [12]. Clausen et al. reported the underestimation of the coordination number in the EXAFS curve fit from the molecular dynamic simulation of a Cu particle [13]. Ryoo et al. also showed the underestimation of the Pt cluster size encapsulated in the supercage of NaY zeolite comparing the results from EXAFS and Xe adsorption measurements [14]. The data analysis of EXAFS for the fresh Ru catalyst faced the same problem as reported earlier. Still, the result of EXAFS supported that the multivalent cation exchanged in the Ru catalyst did not affect the cluster size in the fresh Ru catalyst.

Figure 4 shows the Fourier transforms of the Ru K edge spectra for the oxidized Ru catalysts. The  $\text{La}^{3+}$ - and  $\text{Ce}^{3+}$ -exchanged Ru catalysts had much smaller FT intensity com-

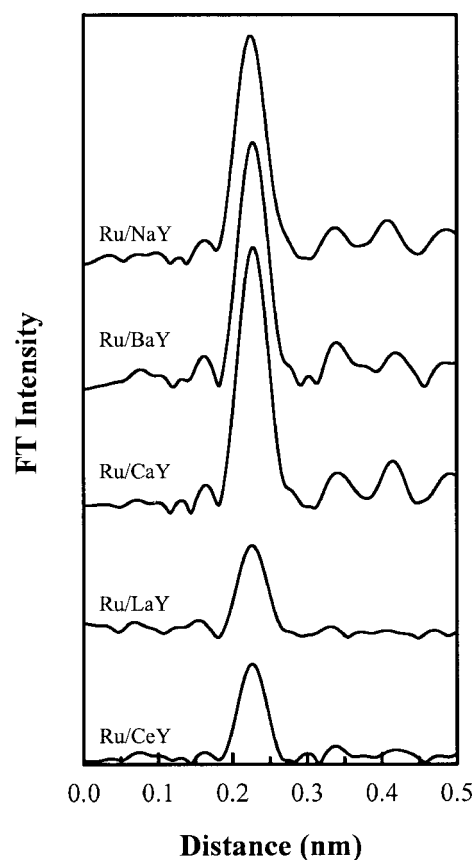


Figure 4. Fourier transforms of the Ru catalyst after the oxidation in 1 atm  $\text{O}_2$  at 573 K and the subsequent reduction with hydrogen flow at 623 K.

pared to other Ru catalysts. The structural parameter, CN, in table 1 suggested the formation of a smaller Ru metal particle, 1 nm according to maximum space filling cluster model. The obtained moderate large Debye–Waller factor indicated a more disordered Ru metal particle, consistent with the formation of a 1 nm Ru cluster. The CN from the  $\text{Na}^{+}$ -,  $\text{Ba}^{2+}$ - and  $\text{Ca}^{2+}$ -exchanged Ru catalysts was consistent with the formation of bulk Ru metal particle. The Debye–Waller factor was the same as that of Ru foil. It was very intriguing that the only trivalent cations suppressed the sintering of Ru metal cluster during the heat treatment in 1 atm  $\text{O}_2$ .

The volatility of Ru metal catalyst for the application of  $\text{NO}_x$  abatement has been explored extensively to stabilize Ru in the matrix of perovskite and perovskite-related ruthenate. The reaction of  $\text{RuO}_2$  with BaO forms  $\text{BaRuO}_3$  which has much lower vapor pressure,  $10^6$  times, as compared to the unpromoted in flowing air at 1450 K [2]. Other useful ruthenates are the perovskites  $\text{SrRuO}_3$  and  $\text{LaRuO}_3$  and the cubic pyrochlore  $\text{Pb}_2\text{Ru}_2\text{O}_{7-\lambda}$  ( $\lambda \approx 1$ ) [15]. The reduction–oxidation of  $\text{CaRuO}_3$  under controlled conditions decreased the size of the obtained Ru metal crystallites [16]. A similar example can be found in  $\text{LaCoO}_3$  and  $\text{LaNiO}_3$  [17]. The alkali or alkaline-earth metal oxide is certainly believed to react with Ru metal to inhibit the sintering by avoiding the formation of volatile  $\text{RuO}_4$  or  $\text{RuO}_3$ .

Trivalent cations,  $\text{La}^{3+}$ ,  $\text{Ce}^{3+}$ , in Y zeolite after complete dehydration do not occupy the ion-exchange site located in

the supercage at ambient temperature [18]. The location of rare-earth cations depends much on the thermal treatments. The calcination of the cation-exchanged faujasite seems to form bulky oxide complexes such as  $[\text{Ce}_2\text{O}_2]^{4+}$ ,  $[\text{Ce}_2(\text{OH})_2]^{2+}$ ,  $[\text{La}_2\text{O}_2]^{2+}$  and  $[\text{La}_2(\text{OH})_2]^{4+}$  preferentially in the supercage, whereas the smaller cations locate in the sodalite cage [19,20]. The large bulky  $\text{La}^{3+}$  and  $\text{Ce}^{3+}$  complexes are able to react with  $\text{RuO}_2$  to form the perovskite-type ruthenate of low vapor pressure, resulting in the smaller Ru metal crystallite after the reduction with hydrogen flow at 623 K. However, most monovalent and divalent cations,  $\text{Na}^+$ ,  $\text{Ba}^{2+}$  and  $\text{Ca}^{2+}$ , after the complete dehydration still occupy the ion-exchange site located in the supercage. Thus, the cation seems not to be available for the formation of perovskite-type ruthenates.

The results in this work suggest that the sintering of Ru metal occurs with the formation of volatile  $\text{RuO}_4$  or  $\text{RuO}_3$  for the  $\text{Na}^+$ -,  $\text{Ba}^{2+}$ - and  $\text{Ca}^{2+}$ -exchanged Y zeolites whereas it occurs with perovskite-type ruthenates for the  $\text{La}^{3+}$ - and  $\text{Ce}^{3+}$ -exchanged Y zeolites. Further work is in progress to elucidate the state of multivalent cations in sintering of metal catalysts.

#### 4. Conclusion

The only trivalent cations,  $\text{La}^{3+}$  and  $\text{Ce}^{3+}$ , affect significantly the size of the obtained Ru particle after the oxidation in 1 atm  $\text{O}_2$ . On the other hand, no effect of the multivalent cations on the formation and the migration of Ru cluster in the supercage of NaY zeolite has been found.

#### References

- [1] J.-G. Kim, S.-K. Ihm, J.Y. Lee and R. Ryoo, *J. Phys. Chem.* 95 (1991) 8546.
- [2] M. Shelef and H.S. Gandhi, *Platinum Metal Review* 18 (1974) 2.
- [3] S.J. Cho, S.M. Jung, Y.G. Shul and R. Ryoo, *J. Phys. Chem.* 96 (1992) 9922.
- [4] J.J. Verdonck, D.A. Jacobs, M. Genet and G. Poncelet, *J. Chem. Soc. Faraday Trans. I* 76 (1980) 403.
- [5] I.H. Cho, S.J. Cho, S.B. Park and R. Ryoo, *J. Catal.* 153 (1995) 232.
- [6] R. Ryoo, J.H. Kwak and L.C. de Mornorval, *J. Phys. Chem.* 98 (1994) 7101.
- [7] R. Ryoo, S.J. Cho, C. Pak, J.-K. Kim, S.-K. Ihm and J.Y. Lee, *J. Am. Chem. Soc.* 114 (1992) 76.
- [8] Q.J. Chen, T. Ito and J. Fraissard, *Zeolites* 11 (1991) 239.
- [9] C. Pak and R. Ryoo, *J. Kor. Chem. Soc.* 36 (1992) 351.
- [10] J.J. Rehr, J. Mustre de Leon, S.I. Zabinsky and R.C. Albers, *J. Am. Chem. Soc.* 113 (1991) 5135.
- [11] (a) P.J. Ellis and H.C. Freeman, *J. Synchrotron Rad.* 2 (1995) 190;  
(b) P.J. Ellis, H.C. Freeman, M.A. Hitchman, D. Reinen and B. Wagner, *Inorg. Chem.* 33 (1994) 1249.
- [12] G. Bunker, *Nucl. Instrum. Methods Phys. Rev.* 207 (1983) 437.
- [13] B.S. Clausen, J. Gråbæk, H. Topsøe, L.B. Hansen, P. Stoltze, J.K. Nørskov and O.H. Nielsen, *J. Catal.* 141 (1993) 368.
- [14] R. Ryoo, S.J. Cho, C. Pak and J.Y. Lee, *Catal. Lett.* 20 (1993) 107.
- [15] R.J.H. Voorhoeve, J.P. Remeika and L.E. Trimble, *Mater. Res. Bull.* 9 (1974) 1393.
- [16] A. Reller, G. Davoodabady, A. Portmann and H.R. Oswald, in: *Proc. 8th Eur. Congr. Electron Microscopy*, Budapest, 1984, p. 1165.
- [17] (a) M. Crespin and W.K. Hall, *J. Catal.* 69 (1981) 359;  
(b) M. Crepin, P. Levitz and L. Gatineau, *J. Chem. Soc. Faraday II* 79 (1983) 1181.
- [18] D.W. Breck, *Zeolite Molecular Sieves – Structure, Chemistry and Use* (Wiley, New York, 1974).
- [19] A.K. Cheetham, M.M. Eddy and J.M. Thomas, *J. Chem. Soc. Chem. Commun.* (1984) 1137.
- [20] R. Carvajal, P.-J. Chu and J.H. Lunsford, *J. Catal.* 125 (1990) 23.